Journal of the European Ceramic Society 22 (2002) 1235–1241
www.elsevier.com/locate/jeurceramsoc

Ultrasonic machining of alumina-based ceramic composites

Deng Jianxin[a,*], Lee Taichiu[b]

[a]Department of Mechanical Engineering, Shandong University, Jinan 250061, Shandong Province, PR China
[b]Department of Manufacturing Engineering, The Hong Kong Polytechnic University, Hung Hom, Kowloon, Hong Kong, China

Received 21 March 2001; received in revised form 8 August 2001; accepted 15 August 2001

Abstract

In ultrasonic machining (USM), the material is removed primarily by repeated impact of the abrasive particles, and the material removal rate (MRR) and surface integrity are influenced by various factors including the material parameters of the workpiece materials. In this study, effect of the properties and microstructure of the workpiece materials on the MRR in ultrasonic machining of alumina-based ceramic composites was investigated. The distributions of strength of the ultrasonic machined specimens were used to evaluate the surface integrity. Results showed that fracture toughness of the ceramic composite played an important role with respect to MRR. In USM of whisker-reinforced alumina composites, the MRR depended on the whisker orientation. Studies of strength distributions of alumina-based ceramic composites machined by USM demonstrated that the flexural strength varied narrowly from the mean value, and the composites with high fracture toughness showed higher Weibull modulus.

Keywords: Al_2O_3; Composites; Machining; Ultrasonic machining

1. Introduction

In contrast to metallic or polymer materials, the machinability of ceramics is very limited. Characteristic ceramic properties, such as high hardness, lack of ductility, and low resistance to thermal shock, often result in low material removal rate (MRR), relatively poor surface quality and subsurface damage, which may grow into a spontaneous fracture during machining. Ultrasonic machining (USM) is an abrasive machining process by which hard and brittle materials can be machined whether conducting or not, and the workpiece experiences no thermal damage. For example, electro-discharge machining and laser beam machining rely strongly on thermal cutting mechanism, and can usually cause a thermally damaged surface layer with micro-cracking.[1–3] In contrast, USM is a non-thermal process, and is especially suited to the machining of ceramic materials, regardless of their electrical conductivity.[4–6]

In USM of ceramics, the material is removed primarily by repeated impact of the abrasive particles. Several studies[7,8] have been shown that impact of brittle materials by hard and sharp particles are generally thought to result from elastic/plastic fracture. This type of fracture is characterized firstly by plastic deformation of the contact area between the impacting particle and the ceramic surface, with subsurface lateral cracks propagating outward from the base of the contact zone on the planes nearly parallel to the surface, and with median cracks propagating from the contact zone normal to the surface. The material removal is thought to occur primarily by surface chipping when lateral cracks curve up and intersect the surface. While the median cracks remain in the surface and influence subsequent strength. Since the formation and propagation of the lateral and median cracks are though to be closely related to the material parameters of the workpiece materials, the MRR, surface integrity, residual strength and its distributions of the ultrasonic machined ceramics would be successively effected by the material parameters of the workpiece materials.

In this study, effect of the properties and microstructure of the workpiece materials on the MRR and surface integrity in ultrasonic machining of alumina-based ceramic composites was investigated. The MRR and surface roughness were examined in relation to the properties and the microstructure. The surface integrity

* Corresponding author.
E-mail address: jxdeng@sdu.edu.cn (D. Jianxin).

0955-2219/02/$ - see front matter
PII: S0955-2219(01)00437-X

was evaluated by measuring the flexural strength and determining its distributions. The purpose was to characterize the effect of the properties and microstructure on the MRR and surface integrity in USM of alumina-based ceramic composites.

2. Materials and experimental procedures

2.1. Preparation and characterization of the alumina-based ceramic composites

The materials used in the present investigation were several hot-pressed alumina-based ceramic composites fabricated by the authors, which provided a reasonably wide range of mechanical properties and microstructure for the study (Table 1). Al_2O_3/TiC, Al_2O_3/TiB_2 and Al_2O_3/(Ti, W)C are of three particle reinforced ceramic composites, Al_2O_3/SiC_w is a whisker reinforced ceramic composite, while $Al_2O_3/TiB_2/SiC_w$ is toughened by incorporation of both particles and whiskers.

A monolithic Al_2O_3 (average particle size 0.5 μm) was used as the baseline material. Additions of TiC, TiB_2, and (Ti, W) C particles (average particle size 0.8 μm) or SiC whiskers (diameter 1–3 μm, length 20–80 μm) were added to $A1_2O_3$ matrix according to the combinations listed in Table 1. The final densification was accomplished by hot pressing with a pressure of 36 MPa in argon atmosphere for 8–60 min to produce a ceramic disk. The required sintering temperature was in the range of 1600–1800 °C.

Test pieces of 3×4×36 mm were prepared from the hot-pressed disks by cutting and grinding using a diamond wheel and were used for the measurement of flexural strength and fracture toughness. A three-point bending mode was used to measure the flexural strength over a 30 mm span at a crosshead speed of 0.5 mm/min. Fracture toughness was determined by the indentation micro-fracture technique. Data for flexural strength and fracture toughness were gathered on five specimens and are listed in Table 1.

Fig. 1 shows microstructure of $A1_2O_3$/TiC ceramic composite, specimens were etched using a hot-solution of phosphoric acid. In this structure, the white phases with clear contrast are of TiC, and the grey phases are of $A1_2O_3$. It can be seen that the second phases were uniformly distributed with the matrix, and there were few second phase agglomerates or matrix-rich regions. Optical micrograph of the polished surfaces perpendicular to the hot pressing direction of Al_2O_3/SiC_w composites is shown in Fig. 2. The white needle-like phases are of SiC whiskers. It is evident that the whiskers were homogeneity dispersed in the matrix.

Table 1
Composition and mechanical properties of alumina-based ceramic composites

Code name	Compositions (vol.%)	Flexural strength (MPa)	Fracture toughness ($MPa.m^{1/2}$)
A	$A1_2O_3$/45% (Ti, W)C	800	4.9
B	$A1_2O_3$/55% TiC	900	5.04
C	$A1_2O_3$/25% TiB_2	780	5.2
D	$A1_2O_3$/20% TiB_2/10% SiC_w	750	7.8
E	$A1_2O_3$/30% SiC_w	760	8.6

2.2. Ultrasonic machining tests

Ultrasonic machining tests were conducted by using a J93025 machine tool (made in China). The schematic diagram of the ultrasonic machine tool is shown in Fig. 3. The ultrasonic generator produces a high frequency electrical signal, which has a power of 250 W and frequency of 16–25 KHz. The electrical signal is transformed into a mechanical vibration signal with the

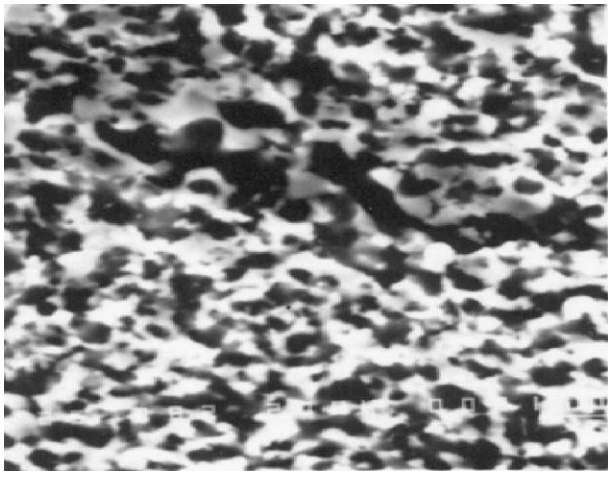

Fig. 1. Microstructure of Al_2O_3/TiC ceramic composite.

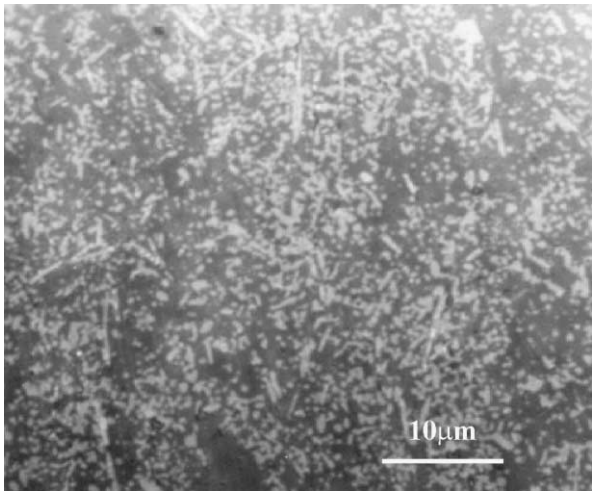

Fig. 2. Optical micrograph of the polished surface perpendicular to the hot-pressing direction of $A1_2O_3/SiC_w$ composite (bar = 10 μm).

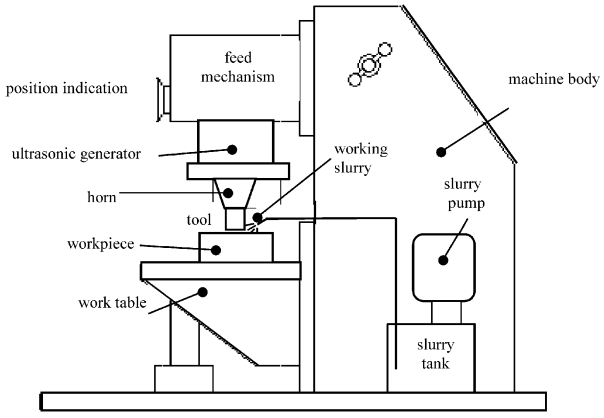

Fig. 3. Schematic diagram of the ultrasonic machine tool (type: J93025).

same frequency by a magnetostrictive nickel-stack transducer. A horn amplifies the signal and transmits it to the tool. The working slurry is supplied under pressure by a single pump. The abrasive was of 80-grit B_4C powders. The specifications of the machine tool and the test conditions are listed in Table 2. The MRR was calculated by dividing the volume removed by the machining time, and expressed in mm^3/min. The surface roughness measurements for the machined specimens were carried out on a talysurf 10 system. The microstructures of the machined surfaces of the ceramic composites were observed by scanning electron microscopy (SEM).

3. Results and discussions

3.1. Effect of properties on the material removal rate and surface roughness

In USM of ceramics, the abrasive particles in slurry with water are under a tool, which is excited by an ultrasonic frequency with small amplitude, and the material is removed by repeated impact of the abrasive particles on the ceramic surface. The material removal by particle impact is thought to occur primarily by surface chipping when lateral cracks curve up and intersect the surface. The most important parameters that control the material removal are identified by indentation fracture mechanics. The general equation for the material removal in brittle materials, especially in ceramics, by impacting particle is

$$V = \sum N\pi C_L^2 h \tag{1}$$

Where V is the volume loss, C_L the lateral crack length, h the mean depth, ΣN the total number of impact particles per unit true particle volume. The lateral crack length and the mean depth are given by[9,10]

$$C_L \propto \left[(E/H_V)^{3/4} K_{IC}^{-1} H_V^{-1/4}\right]^{1/2} P^{5/8} \tag{2}$$

$$h \propto (E/H_V)^{1/2} (P/H_V)^{1/2} \tag{3}$$

Where E and H_V are elastic modulus and the Vicker's hardness of the materials, and P is the mean vertical impact force acting from one particle to material during machining. It can be seen from Eqs. (2) and (3) that the size of the lateral and median crack grows with a decrease in the fracture toughness and an increase in the load.

Fig. 4 shows the mutual dependence of fracture toughness and the material removal rate in USM of different alumina-based ceramic composites. The surfaces perpendicular to the hot pressing direction of the whisker reinforced ceramic composites ($A1_2O_3/SiC_w$ and $A1_2O_3/TiB_2/SiC_w$) were chosen for the machining surface. It can be seen that the fracture toughness played an important role on the MRR. The composites with high fracture toughness showed lower MRR. The whisker reinforced ceramic composites had the smaller MRR, while the particle reinforced ceramic composites showed the higher MRR. This can be explained by an energy consideration. The fracture toughness of a material is a measure of the energy required to make a crack grow, and the composites with high fracture toughness need more energy. Under identical machining conditions, the energy input is kept as constant, therefore, the only way to put more energy into the machining process is to increase the machining time (or to decrease

Table 2
Specifications of the USM machine tool and the test conditions

Nominal output power	250 (W)
Frequency	16–25 (kHz)
Amplitude of vibration	5–20 (μm)
Static load	10 (N)
Tool material	Mild steel (Φ5)
Abrasive particle	B_4C (80 grit)

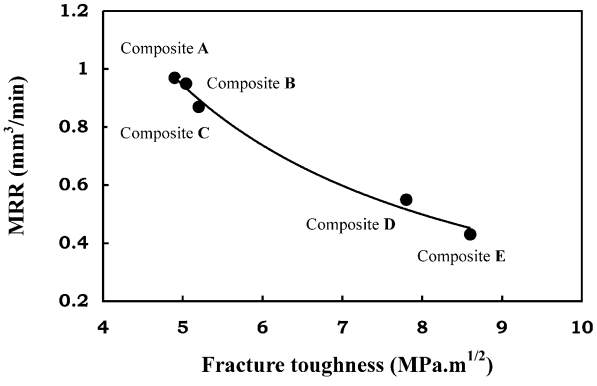

Fig. 4. Material removal rate in ultrasonic machining of different alumina-based ceramic composites.

the MRR). Fig. 5 shows the surface roughness in USM of these alumina-based ceramic composites. It can be seen that there is a similar tendency with that of the MRR, the most productive materials give the greatest roughness and vice versa. Similar observations have been reported for several single-phase ceramics.[11]

3.2. Effect of microstructure on the material removal rate and surface roughness

Hot-pressed whisker reinforced ceramic composites induce an anisotropy in whisker distribution and lead to the composite with an orientation dependance of the mechanical properties and performance.[12,13] Therefore, the material removal rate in USM of this kind of ceramic composite would be influenced by the whisker orientation. Fig. 6 shows the effect of whisker orientation on the MRR in ultrasonic machining of $A1_2O_3/SiC_w$ and $A1_2O_3/TiB_2/SiC_w$ ceramic composites. Where θ represents the direction angles of the machined surface to the surface normal to the hot pressing direction as can be seen in reference.[12] It is evident that the whisker orientation played an important role on the MRR. As the direction angle θ ranged from 0 to 90°, a decrease in MRR was observed. The $\theta=90°$ surface had the smallest MRR, and the $\theta=0°$ surface showed the highest MRR. Fig. 7 shows the effect of whisker orientation on the surface roughness in USM of $A1_2O_3/SiC_w$ and $A1_2O_3/TiB_2/SiC_w$ composites. It can be seen that the effect of whisker orientation on the surface roughness had a similar outline with that of on the MRR. The $\theta=90°$ surface exhibited the lowest surface roughness for each composite.

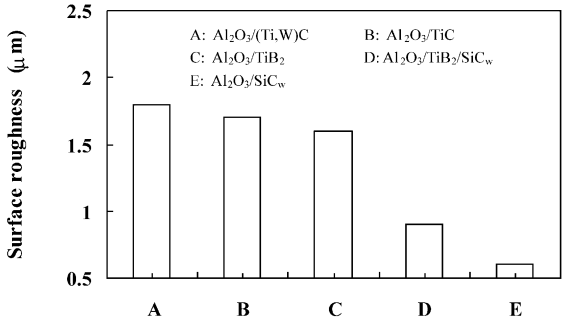

Fig. 5. Machined surface roughness in ultrasonic machining of different alumina-based ceramic composites.

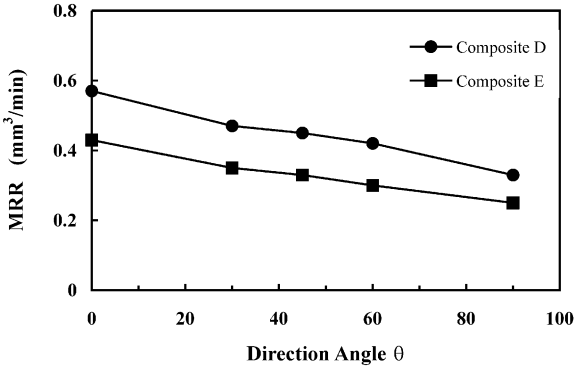

Fig. 6. Material removal rates vs. direction angle θ in ultrasonic machining of whisker reinforced ceramic composites.

Fig. 8 illustrates schematically the interactions between the lateral crack caused by impact particles and the whiskers, which occurred in each case respectively. For $\theta=0°$ surface, most of the whiskers were distributed parallel to the machining surface, the lateral crack caused by the impact particles propagated in the direction parallel to the whisker plane (Fig. 8a). The whiskers no longer shared the load, and bridging rarely occurred. Little or no whisker toughening took place since lateral crack could readily propagate through the matrix. Hence, it can be stated that for this type of machining, the whiskers cannot support any applied stresses and act as effective toughening elements. So in this case, larger MRR was observed. SEM micrograph of ultrasonically machined $A1_2O_3/SiC_w$ surfaces with $\theta=0°$ are shown in Fig. 9. It can be seen that a lot of whisker-like deep microgrooves existed on the machined surface. These whisker-like deep microgrooves indicated of the whisker debonding, which provided sufficient evidence that little or no whisker pullout and bridging took place during this type of machining.

Changes in direction angle of the inclined whisker plane to the crack propagation direction influenced the contributions to toughening from bridging, pullout and crack deflection. When the direction angle θ between the whisker plane and the lateral crack propagation direction was changed from $\theta=0$ to 90°, for example $\theta=45°$ (Fig. 8b), the crack propagation direction was not normal to the whisker plane. In this case, the whiskers experienced both tensile and bending stresses, and there was an increased probability of whisker fracture because of the bending force on the whiskers. While for $\theta=90°$ surface, most of the whiskers were distributed normal to machining surface, the lateral crack caused by the impact particles propagated in the direction perpendicular to the

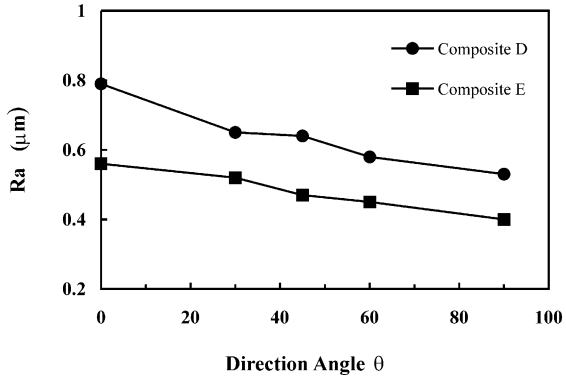

Fig. 7. Machined surface roughness vs. direction angle θ in ultrasonic machining of whisker reinforced ceramic composites.

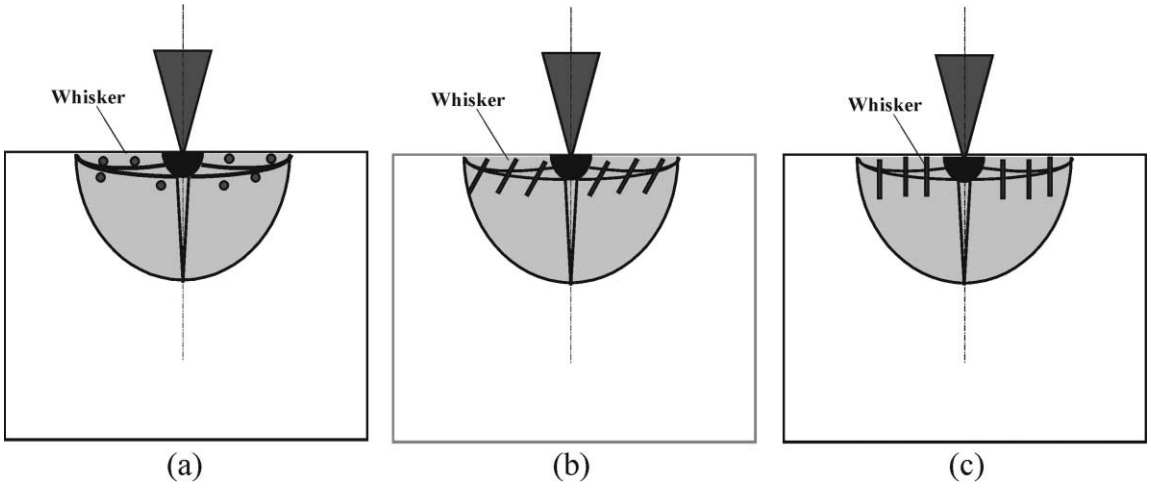

Fig. 8. Schematic illustration of the interactions between the abrasive particles and the whiskers of specimens when (a) $\theta = 0^\circ$, (b) $\theta = 45^\circ$ and (c) $\theta = 90^\circ$ surface are used as the machining surface in ultrasonic machining.

whisker axis (Fig. 8c), the whisker experienced tensile stresses. The bridging whiskers imposed closure stress at the crack tip, acted as the major load-bearing element and resisted the crack propagation. Thus in the case of $\theta = 90^\circ$, the whiskers could be loaded to a greater extent than that of other cases, and the resistance to whisker pullout dissipated energy and was, therefore, the main cause of lowest MRR during this type of machining. The SEM micrograph of the machined surface with $\theta = 90^\circ$ are indicated in Fig. 10. When compared with Fig. 9, there were few whisker-like deep microgrooves on the machined surface.

3.3. Surface integrity of ultrasonic machined alumina-based ceramic composites

The strength of ceramic materials depends on both its inherent resistance to fracture and the stochastically distributed defects such as grain boundaries, pores and cracks, which can lead to large variations in strength. Fracture analysis have shown that the mechanisms responsible for the failure of ceramics are in most cases surface defects, which are often originated during mechanical treatment in the final machining. This machining damage on the surface limits the strength and determines the strength distribution since it influences crack growth under stress.[14,15] It is quite common to observe that fracture strength varies significantly among different specimens of the same material. This is partly due to the randomly distributed surface damages. For this reason, a statistical measure is required to account for its variability. Several studies[16–18] have shown that the Weibull modulus of flexural strength can be used to characterize the surface integrity of the machined ceramics. As the Weibull modulus describes

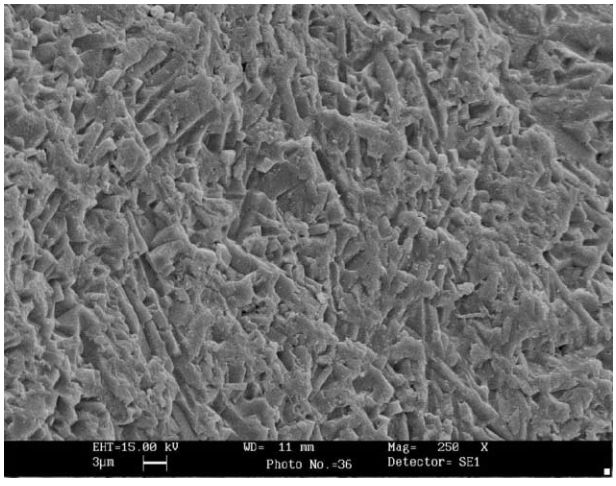

Fig. 9. SEM micrograph of the ultrasonic machined surfaces of Al_2O_3/SiC_w ceramic composite with the surface perpendicular to the hot pressing direction as the machining surface ($\theta = 0^\circ$).

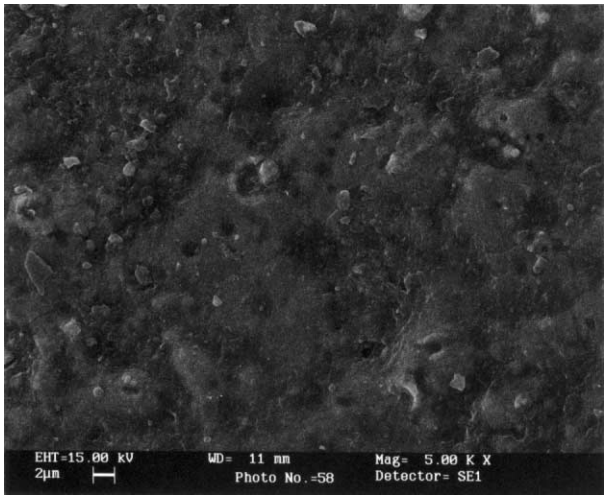

Fig. 10. SEM micrograph of the ultrasonic machined surfaces of Al_2O_3/SiC_w ceramic composite with the surface parallel to the hot pressing direction as the machining surface ($\theta = 90^\circ$).

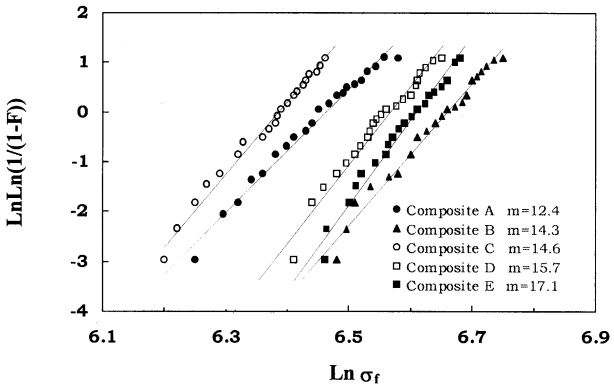

Fig. 11. Weibull plot of the strength distribution of the ultrasonic machined alumina-based ceramic composites.

the distribution of individual values of the flexural strength within a population. A high value of Weibull modulus implies a narrow distribution of strength, and denotes a good material with a high degree of homogeneity of properties. Whereas low Weibull modulus indicates that the distribution of the strength-controlling crack size is broader, which may be resulted from surface damages during the final machining. So the Weibull modulus was used as a parameter characterizing the surface integrity of the ultrasonic machined ceramic composites in this study.

Test pieces of $3\times4\times16$ (mm) were prepared from the sintered disks for the measure of flexural strength. Three-point-bending mode was used to measure the flexural strength over a 10 mm span at a crosshead speed of 0.5 mm/min. The surfaces endured tensile stresses were treated by ultrasonic machining for three minutes. A minimum of 10 specimens from each composite was tested. The strengths were then analyzed by two-parameter Weibull distribution. Fig. 11 shows the Weibull plot of strength distributions of the ultrasonic machined alumina-based ceramic composites. It can be seen that the whisker-reinforced composites showed higher Weibull modulus than that of the particle reinforced composites. The Weibull modulus of the ultrasonic machined ceramic specimens is in the range of 12.4–17.1, and the composites with high fracture toughness showed higher Weibull modulus. The narrow range of strength distribution (or high Weibull modulus) for the ultrasonic machined ceramic composites suggests that there are little strength-limiting damages to the machined ceramic surfaces. Fig. 12 shows the SEM micrographs of the ultrasonic machined surfaces of Al_2O_3/TiB_2 and Al_2O_3/TiC ceramic composites. They exhibited a relative smooth surface, irregularities produced by fracture damage cannot be clearly observed, and there is no distinct crack on the machined surface.

4. Conclusions

1. The fracture toughness plays an important role with respect to MRR and surface roughness in USM of alumina-based ceramic composites. As the fracture toughness increases, there is a reduction in MRR and in surface roughness.
2. In USM of whisker reinforced ceramic composites, the MRR and the surface roughness depend on the whisker orientation, and vary on surfaces with different direction angle θ normal to the hot pressing direction. This can be well explained by the lateral crack fracture model. For $\theta=0^\circ$ surface, little or no whisker toughening takes place since the whiskers share no load, lateral crack can readily propagate through the matrix. While for $\theta=90^\circ$ surface, the bridging whiskers impose closure stress at the crack tip and resist the crack propagation.
3. Studies of strength distributions of alumina-based composites machined by USM demonstrate that the flexural strength of the ultrasonic machined specimens varies narrowly from the mean value, and the composites with high fracture toughness show higher Weibull modulus.

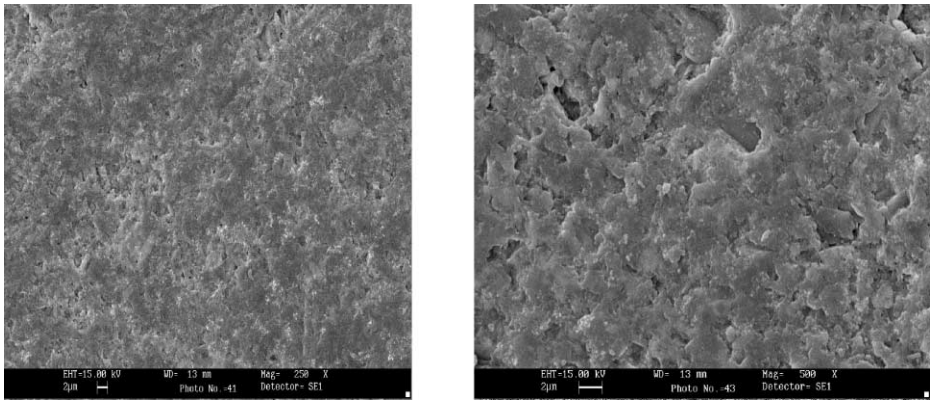

Fig. 12. SEM micrographs of the ultrasonic machined surfaces (a) Al_2O_3/TiB_2, and (b) Al_2O_3/TiC ceramic composites.

Acknowledgements

This work described in this paper has been supported by the Research Grants Council of Hong Kong, China (PolyU 5173/97E)

References

1. Petrofes, N. F. and Gadalla, A. M., Electrical discharge machining of advanced ceramics. *American Ceramic Society Bulletin*, 1998, **67**(6), 1048–1052.
2. Deng, J. and Lee, T., Surface integrity in electro-discharge machining, ultrasonic machining, and diamond saw cutting of ceramic composites. *Ceramics International*, 2000, **26**, 825–830.
3. Tönshoff, H. K. and Emmelmann, C., Laser cutting of advanced ceramics. *Annals of the CIRP*, 1989, **38**(1), 219–226.
4. Thoe, T. B., Aspinwall, D. K. and Wise, M. L. H., Review on ultrasonic machining. *International Journal of Machine Tools Manufacturing*, 1998, **38**(4), 239–255.
5. Hahn, R. and Schulze, P., Ultrasonic Machining of glass and ceramics. *American Ceramic Society Bulletin*, 1993, **72**(8), 102–106.
6. Kumabe, J., Ultrasonic superposition vibration cutting of ceramics. *Precision Engineering*, 1989, **11**(2), 71–76.
7. Lawn, B. R., Evans, A. G. and Marshall, D. B., Elastic/plastic indentation damage in ceramics: the median/radial crack system. *Journal of American Ceramic Society*, 1980, **63**(9–10), 574–1581.
8. Marshall, D. B., Lawn, B. R. and Evans, A. G., Elastic/plastic indentation damage in ceramics: the lateral crack system. *Journal of American Ceramic Society*, 1982, **65**(11), 561–566.
9. Wiederhorn, S. W. and Hockey, B. J., Effect of material parameters on the erosion resistance of brittle material. *Journal of Material science*, 1983, **18**, 766–780.
10. Kamiya, H., Sakakibara, M. and Sakurai, Y., Erosion wear properties of tetragonal ZrO_2 (Y_2O_3)—toughened Al_2O_3 composites. *Journal of American Ceramic Society*, 1994, **77**(3), 666–672.
11. Dam, H. and Quist, P., Productivity, surface quality and tolerances in ultrasonic machining of ceramics. *Journal of Materials Processing Technology*, 1995, **51**, 358–368.
12. Jianxin, D. and Xing, A., Effect of whisker orientation on the friction and wear behaviour of $A1_2O_3/TiB_2/SiC_w$ composites in sliding wear tests and in machining processes. *Wear*, 1996, **201**, 178–185.
13. Lee, F. and Sandlin, M. S., Toughness anisotropy in textured ceramics. *Journal American Ceramic Society*, 1993, **76**(6), 1793–1800.
14. Tönshoff, H. K. and Trumpold, H., Evaluation of surface layers of machined ceramics. *Annals of the CIRP*, 1989, **38**(2), 699–708.
15. Li, K. and Warren Liao, T., Surface/subsurface damage and the fracture strength of ground ceramics. *Journal of Materials Processing Technology*, 1996, **57**, 207–220.
16. Schubert, E. and Bergmann, H. W., Surface modification of ceramic materials using excimer lasers. *Surface Engineering*, 1993, **9**(1), 77–81.
17. Jianxin, D. and Taichiu, L., Techniques for improved surface integrity and reliability of machined ceramic composites. *Surface Engineering*, 2000, **16**(5), 411–414.
18. Lee, T. C. and Zhang, J. H., Surface treatment of wire electro-discharge machined engineering ceramics by abrasive blasting. *Journal of Adhesion Science and Technology*, 1998, **12**(6), 585–592.